RESEARCH ON PHOTONIC CRYSTAL FIBERS USING FINITE DIFFERENCE ELECTROMAGNETIC ANALYSIS

Chin-ping Yu[(1)] **and Hung-chun Chang**[(2)]

[(1)] *Graduate Institute of Communication Engineering,*
National Taiwan University, Taipei, Taiwan 106-17, Republic of China
E-mail: f86025@ew.ee.ntu.edu.tw

[(2)] *Department of Electrical Engineering, Graduate Institute of Electro-Optical Engineering,*
and Graduate Institute of Communication Engineering
National Taiwan University, Taipei, Taiwan 106-17, Republic of China
E-mail: hcchang@cc.ee.ntu.edu.tw

ABSTRACT

Photonic crystal fibers (PCFs) are one successful application of the photonic crystal concept. We report on analysis and design of the PCFs using the finite difference mode solver. The full-vectorial characteristics of PCFs, including the effective indexes and field distributions of the guided modes, are obtained. Both PCFs based on the total internal reflection guiding mechanism ("holey fibers") and those resulting from photonic bandgap effect have been studied. For the holey fibers, the dispersion property is calculated and is shown to agree very well with experimental values. The vectorial modes on PCFs with a large air core are accurately analyzed.

INTRODUCTION

Photonic crystal fibers (PCFs) or microstructured fibers are novel photonic structures that represent one successful application of the photonic crystal concept [1], [2]. In recent years many research efforts have been devoted to understanding the propagation characteristics of such fibers, based on different theoretical methods [3]–[6], and to demonstrating their possible applications. In this paper we report on analysis and design of the PCFs using the finite difference mode solver. We demonstrate that the full-vectorial finite difference method that has often been employed to study waveguide modes of various dielectric waveguides [7] can be efficiently used to obtain the propagation characteristics, including the effective indexes and field distributions, of different PCFs.

The first PCF reported in 1996 [1] was made from undoped fused silica having a hexagonal array of air holes along its length, with the central hole missing, forming a core area. The scanning electron microscopic (SEM) picture and the cross-section of a typical PCF are shown in Fig. 1(a) [8] and (b), respectively. It was understood that light can be guided

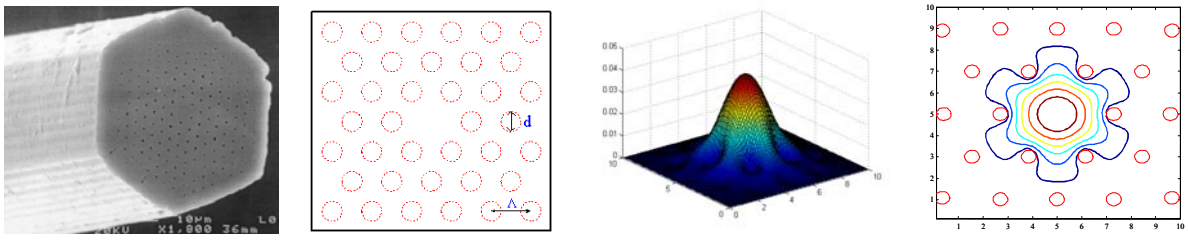

(a) (b) (c) (d)

Fig. 1. (a) SEM picture of the PCF [8]. (b) The cross-section of the PCF. (c) The field distribution and (d) the transverse field distribution for the x-polarized guided mode of the PCF at $\lambda = 0.6328$ μm with $d = 0.6$ μm.

on such structure because the refractive index of the core area is higher than the effective index of the surrounding air-hole array, making the required total internal reflection possible. One peculiar feature of the PCF is that it can maintain as a single-mode guide over a wide wavelength range, called "endlessly single-moded" [2]. In contrast to the

[†]This work was supported in part by the National Science Council of the Republic of China under Grant NSC90-2215-E-002-040.

effective total internal reflection guiding of the holey fibers, light guiding in the core area due to the existence of photonic bandgaps (PBGs) in the cladding region has been achieved in PCFs in which the core index is made smaller than the effective index of the cladding region [9], and even in PCFs with a large air core [10]. Vectorial modes of all these fibers will be calculated and discussed in this paper.

THE FINITE DIFFERENCE MODEL

Starting from Maxwell's equations, the vector wave equation in a linear, isotropic, and time-invariant medium is derived as

$$\nabla \times \nabla \times \overrightarrow{E} = \nabla(\nabla \cdot \overrightarrow{E}) - \nabla^2 \overrightarrow{E} = n^2 k_0^2 \overrightarrow{E} \tag{1}$$

where n is the refractive index as a function of position, and $k_0 = 2\pi/\lambda_0$ is the wave number in free space. For the refractive index does not vary along the z direction, the propagation of the electromagnetic wave is governed by two coupled equations for E_x and E_y only. By writing the electric field as $\overrightarrow{E} = (E_x \hat{x} + E_y \hat{y} + E_z \hat{z}) \exp(-j\beta z)$, where β is the propagation constant, and considering only the transverse part of the field, we can obtain an eigenvalue equation of the form [11]

$$\begin{bmatrix} A_{xx} & A_{xy} \\ A_{yx} & A_{yy} \end{bmatrix} \cdot \begin{bmatrix} E_x \\ E_y \end{bmatrix} = \beta^2 \begin{bmatrix} E_x \\ E_y \end{bmatrix}. \tag{2}$$

The cross-section of a PCF is then discretized into many mesh points with the above Maxwell differential equations using the central difference scheme to form a set of elementary matrix equations. The effective indexes of the guided modes are obtained by finding out the eigenvalues of the matrix equations, and the field distributions from solving for the eigen vectors. Since the guided modes are found well centrally confined, the computational window is not necessarily large and the transparent boundary condition [11] has been utilized at its boundary.

NUMERICAL RESULTS

We first analyze the PCF that has the radius of the core region equal to Λ , the distance between two air hole centers. The field distribution in the PCF is shown in Fig. 1(c) and (d) at $\lambda = 0.6328$ μm with $d = 0.6$ μm, where d is the air hole diameter. The field is seen to be confined very well in the core area for the air holes reduce the refractive index of the cladding region. Smaller holes also make single-mode guidance more likely. Fig. 2(a) shows the mode indexes of the guided modes versus the normalized frequency with $d/\Lambda = 0.3$. There are actually two modes with different polarization states, which are too close to be distinguished from each other in the figure. The PCF is thus considered as single-moded over a remarkably large band of frequency. Our result agrees very well with previous experimental results [2]. If we further increase the hole diameter, the gaps between the holes become narrower, isolating the core more strongly from the silica in the cladding. Thus, there will be more guided modes in the PCF, as shown in Fig. 2(b) with $d/\Lambda = 0.5$.

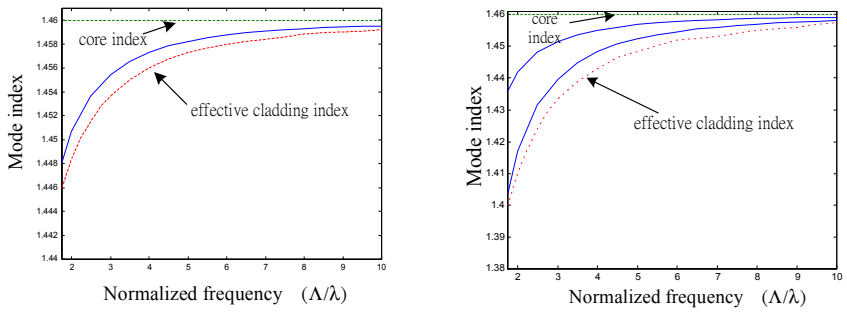

(a) (b)

Fig. 2. Modal dispersion curves for (a) a single-mode PCF with $d/\Lambda = 0.3$ and (b) a multimode PCF with $d/\Lambda = 0.5$.

Fig. 3(a) shows the transverse field distribution of the guided mode in the PCF with $d = 1.4$ μm at $\lambda = 0.6328$ μm. Compared with Fig. 1(d), we can see that the field is more centrally located for larger air-hole diameter for it reduces more the cladding index, increasing the index difference between the core and cladding regions. At shorter wavelengths the field becomes more concentrated in the silica regions and avoids the holes as shown in Fig. 1(d) at $\lambda = 0.6328$ μm. As for

larger wavelengths, the field will extend more into the holes and the cladding region, as shown in Fig. 3(b) at $\lambda = 1.55$ μm.

The dispersion properties can also be obtained by calculating the effective indexes n_{eff} of the guided modes over a range of wavelength. The actual index of the pure silica is taken into account by means of four-term Sellmeier formulae [12], [13]. The dispersion is derived according to the definition $D = -\lambda d^2 n_{eff}/cd\lambda^2$ considering both the material and the waveguide dispersions. Fig. 4 presents the dispersion characteristics of the PCFs with different air-hole diameters while Λ is set to be 2.3 μm. Note that in our computation for the case with $d = 0.621$ μm and $\lambda = 0.813$ μm, the dispersion is -74.5 ps/nm/km and its slope is 0.472 ps/nm-km/nm, whereas the experimental values in [8] were -77.7 ps/nm/km and 0.464 ps/nm.km/nm, respectively [14]. Our results have very good agreement with the experimental values, showing the reliability of our model. We can also see that the zero-dispersion point can be easily shifted to desired wavelength by changing the geometrical parameters of the PCFs.

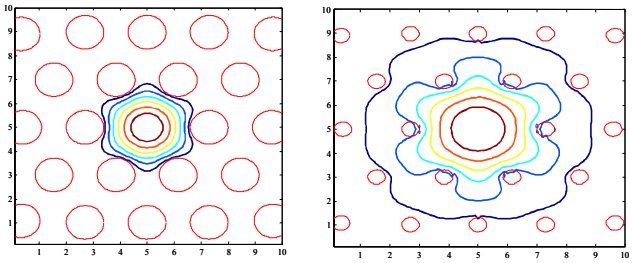

(a) (b)

Fig. 3. The transverse field distribution for the x-polarized guided mode of the PCF at (a) $\lambda = 0.6328$ μm with $d = 1.4$ μm, and (b) $\lambda = 1.55$ μm.

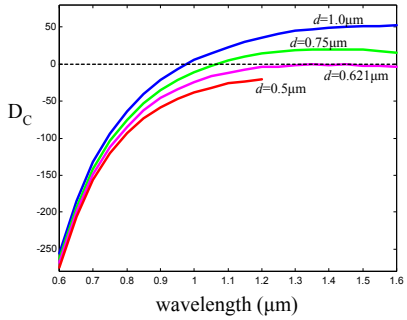

Fig. 4. Dispersion computed versus wavelength for PCFs with different air-hole diameters.

We now consider PCFs with light guiding in the core area due to the existence of PBGs in the cladding region. Fig. 5(a) [9] shows an example of such PCFs, called the honeycomb PCF, which has a smaller air-hole defect in the fiber center resulting in a decrease of the core index. The circles in Fig. 5(b) are the fundamental guided mode indexes on the honeycomb PCF obtained by our model with dashed lines being the boundaries of the PBGs, and the dotted line being the radiation line. The solid line is obtained by the plane-wave expansion method [4], and the triangles are obtained by the FDTD method [6]. Our results appear to be closer to those of the plane-wave expansion method. Another example is the vacuum or air waveguide, as shown in Fig. 6(a) [10]. The core region is filled with air, resulting from removing seven silica glass capillary canes in the fabrication. The fundamental guided modes for $\lambda = 0.55$ μm and $\lambda = 0.65$ μm are shown in Fig. 6(b) and (c), respectively. The field is confined very well in the core area at $\lambda = 0.55$ μm even when the index of the cladding is larger than the index of the core which is equal to 1. The calculated effective mode index is 0.9994993. At $\lambda = 0.65$ μm, the field is seen to spread into the cladding region.

CONCLUSION

We have demonstrated that the finite difference method is an efficient method for studying PCFs. The characteristics of various PCFs, including the effective indexes and the field distributions of the vectorial guided modes, have been calculated and discussed. Dispersion properties of the PCFs can also be obtained by our model, and those for the holey fiber are shown to agree very well with the reported experimental values. We have also successfully analyzed PCFs resulting from pure PBG mechanism.

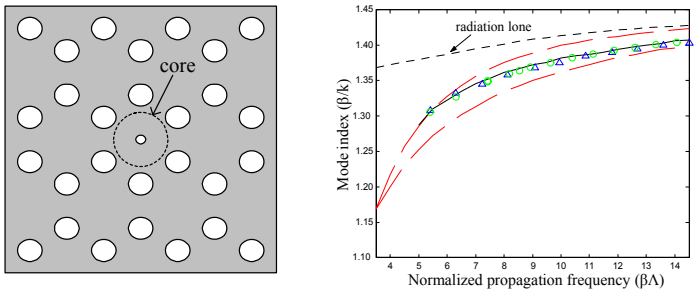

(a) (b)

Fig. 5. (a) Geometry [9] and (b) the fundamental guided mode index of the honeycomb PCF.

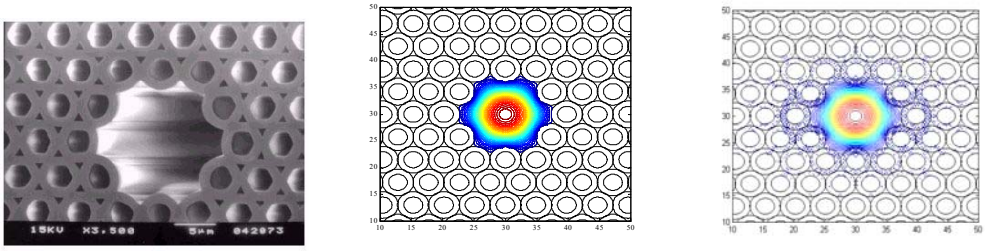

(a) (b) (c)

Fig. 6. (a) SEM picture of a vacuum-guiding PCF [10]. (b) The transverse field distribution for the fundamental guided modes of the vacuum-guiding PCF at $\lambda = 0.55$ μm. (c) Same as (b) but at $\lambda = 0.65$ μm.

REFERENCES

[1] J. C. Knight, T. A. Birks, P. St. J. Russel, and D. M. Atkin, "All-silica single-mode optical fiber with photonic crystal cladding," *Opt. Lett.*, vol. 21, pp. 1547–549, 1996.

[2] J. C. Knight, T. A. Birks, and P. St. J. Russel, "Endlessly single-mode photonic crystal fiber," *Opt. Lett.*, vol. 22, pp. 961–963, 1997.

[3] T. M. Monro, D. J. Richardson, N. G. R. Broderick, and P. J. Bennett, "Holy optical fibers: An efficient modal model," *J. Lightwave Technol.*, vol. 17, pp. 1093–1102, 1999.

[4] S. E. Barkou, J. Broeng, and A. Bjarklev, "Silica-air photonic crystal fiber design that permits waveguiding by a true photonic bandgap effect," *Opt. Lett.*, vol. 24, pp. 46–48, 1999.

[5] F. Brechet, J. Marcou, D. Pagnoux, and P. Roy, "Complete analysis of the characteristics of propagation into photonic crystal fibers, by the finite element method," *Opt. Fiber Technol.*, vol. 6, pp. 181–191, 2000.

[6] M. Qiu, "Analysis of guided modes in photonic crystal fibers using the finite-difference time-domain method," *Microwave and Optical Technol. Lett.*, vol. 30, pp. 327–330, 2001.

[7] Huang, W. P., and C. L. Xu, "Simulation of three-dimentional optical waveguides by a full-vector beam propagation method," *IEEE. J. Quantum.*, vol. 29, pp. 2639–2649, 1993.

[8] Homepage of the Optoelectronics Group, Department of Physics, University of Bath.

[9] J. C. Knight, J. Broeng, T. A. Birks, and P. St. J. Russell, "Photonic band gap guidance in optical fibers," *Science*, vol. 282, pp. 1476–1478, 1998.

[10] R. F. Cregan, B. J. Mangan, J. C. Knight, T. A. Birks, P. St. J. Russell, P. J. Roberts, and D. C. Allan, "Single-mode photonic band gap guidance of light in air," *Science*, vol. 285, pp. 1537–1539, 1999.

[11] G. R. Hadley, "Transparent boundary condition for the beam propagation method," *IEEE J. Quantum Electron.*, vol. 28, pp. 963–970, 1992.

[12] B. Brixner, "Refractive-index interpolation for fused silica," *J. Opt. Soc. Amer.*, vol. 57, pp. 674–676, 1967.

[13] I. H. Maliston, "Interspecimen comparison of the refractive index of fused silica," *J. Opt. Soc. Amer.*, vol. 55, pp. 120–1209, 1965.

[14] M. J. Gander, R. McBride, J. D. C. Jones, D. Mogilevtsev, T. A. Birks, J. C. Knight, and P. St. J. Russel, "Experimental measurement of group velocity dispersion in photonic crystal fibres," *Electron. Lett.*, vol. 35, pp. 63–65, 1999.